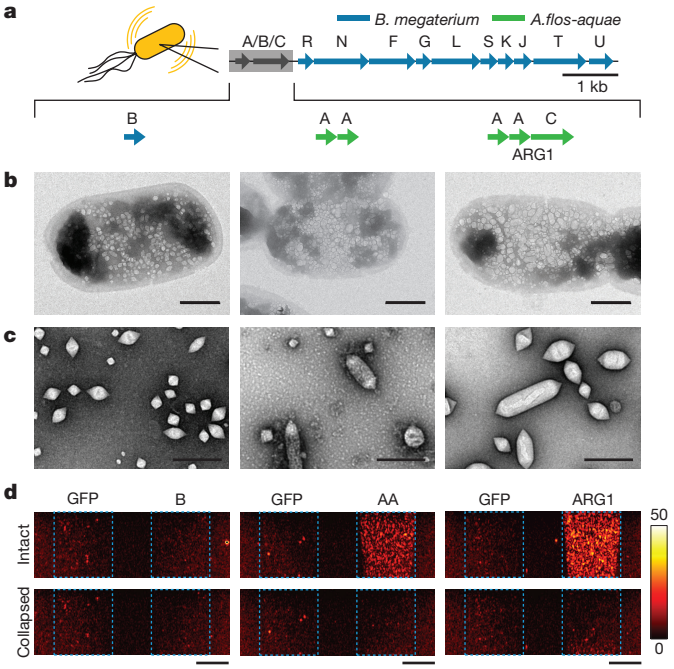

Figure 1 | Genetic engineering of acoustic reporter genes. **a**, Organization of acoustic reporter gene clusters; the region highlighted in grey was varied. Panels **b**–**d** are organized in columns that correspond to each of the variant constructs. **b**, TEM images of representative *E. coli* cells expressing each construct. **c**, TEM images of gas vesicles isolated from *E. coli* expressing each construct. **d**, Ultrasound images of agarose phantoms containing *E. coli* expressing each construct or GFP. The cell concentration is 10^9 cells ml^{-1}. Images in the bottom panels were acquired after acoustic collapse. Dotted blue outlines indicate the location of each specimen. Colour bar represents linear signal intensity. Scale bars, 500 nm (**b**), 250 nm (**c**) and 2 mm (**d**). All imaging experiments were repeated three times with similar results.

regulated by the chemical inducer isopropyl-β-D-thiogalactoside (IPTG). Ultrasound signals from *E. coli* expressing ARGs in this configuration followed the expected dose–response curve of IPTG-controlled expression (Fig. 2c, d), confirming their ability to serve as the output signal for engineered genetic circuits. Significant ultrasound contrast could be observed 4 h after IPTG induction ($P = 0.01$, $n = 4$),

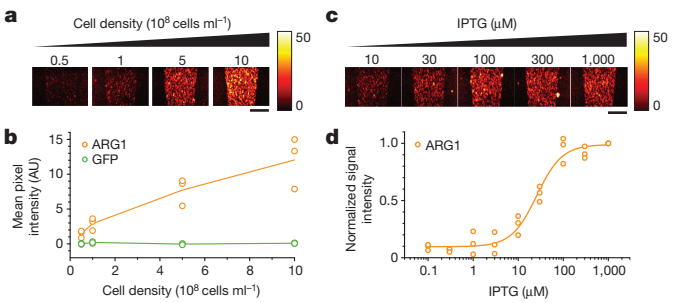

Figure 2 | Imaging dilute bacterial populations and dynamically regulated gene expression. **a**, Ultrasound images of *arg1*-expressing *E. coli* at various cellular concentrations, before and after acoustic collapse. **b**, Mean ultrasound contrast from *E. coli* expressing *arg1* and GFP at various cell densities. Data are from three biological replicates, lines indicate the mean. AU, arbitrary units. **c**, Ultrasound images of *E. coli* expressing *arg1* after induction with various concentrations of IPTG. Cell concentration was 5×10^8 cells ml^{-1}. **d**, Normalized ultrasound contrast as a function of IPTG concentration. Data are from three biological replicates, line shows a fit of the data with the Hill equation to facilitate visualization. Each imaging experiment was repeated three times with similar results. Scale bars, 2 mm.

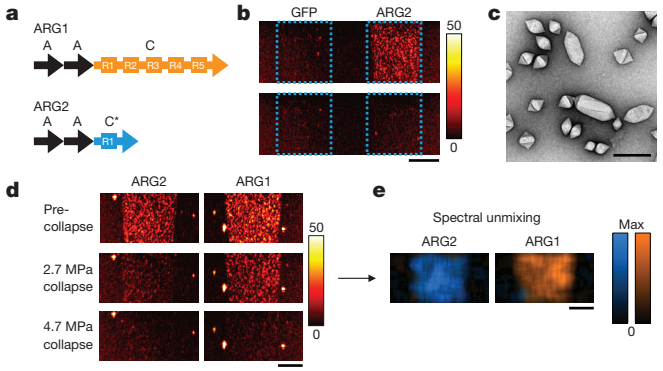

Figure 3 | Multiplexed imaging of genetically engineered reporter variants. **a**, Diagram of the *gvpA* and *gvpC* sequences included in the *arg1* and *arg2* gene clusters. **b**, Ultrasound images of a gel phantom containing *E. coli* expressing GFP or *arg2* (10^9 cells ml^{-1}). Dotted blue outlines indicate the location of each specimen. **c**, TEM images of isolated *arg2* gas vesicles. **d**, Ultrasound images of gel phantoms containing *arg1* or *arg2* before collapse, after collapse at 2.7 MPa and after collapse at 4.7 MPa (10^9 cells ml^{-1}). **e**, Overlay of the blue and orange maps from spectral unmixing of *arg2* and *arg1*, based on the series of images in **d**. Scale bars, 2 mm (**b**, **d**, **e**) and 250 nm (**c**). Each imaging experiment was repeated three times with similar results.

and continued to increase during the 22-h culturing period (Extended Data Fig. 3).

To determine whether the expression of ARGs has any deleterious effect on host cells, we measured the growth curves of *E. coli* expressing *arg1* or GFP. After induction, cells expressing both constructs continued to divide and reached similar saturation densities (Extended Data Fig. 4a). For both *arg1* and GFP, the final density was lower than in uninduced controls, as expected from the metabolic demand of protein expression[22]. We also assessed the viability of ARG-expressing cells after ultrasound imaging and acoustic collapse. Transmission electron microscopy (TEM) images of cells acquired before and after exposure to collapsing acoustic pulses show that gas vesicles can be eliminated without any obvious cellular damage (Extended Data Fig. 4b). To examine the effect of ultrasound exposure on cell growth, we cultured *E. coli* expressing *arg1* as colonies on solid medium and applied acoustic collapse pulses to half of the agar plate. The collapse of gas vesicles in insonated cells was confirmed by a decrease in optical scattering (Extended Data Fig. 4c, d). After incubation for an additional 20 h, no significant difference was observed in the diameter of the insonated colonies compared to un-insonated controls, indicating that ultrasound exposure does not affect cell viability (Extended Data Fig. 4e). Notably, insonated colonies re-expressed gas vesicles during this period, as indicated by the restoration of pressure-sensitive light scattering (Extended Data Fig. 4e, f).

It is often informative to image more than one population of cells simultaneously, as done optically using spectrally distinct fluorescent proteins. Analogous acoustic multiplexing can be performed using genetic variants of gas vesicles that collapse at different pressures using multiple images acquired during sequential application of increasing pressure pulses[20] (Supplementary Note 1). To explore whether this could be done with ARGs, we constructed a new version of the ARG-expressing gene cluster containing a modified version of *A. flos-aquae gvpC*. Deletion or truncation of this outer scaffolding protein results in gas vesicles with lower collapse pressures[23], allowing the production of nanostructures that are distinguishable from each other under ultrasound[20]. Using this approach, we modified our gene cluster by truncating GvpC to retain only one of its five repeating α-helical domains (Fig. 3a). *E. coli* expressing the resulting gene cluster, which we refer to as *arg2*, showed robust production of gas vesicles and ultrasound contrast, similar to *arg1* (Fig. 3b, c and Extended Data Fig. 5a–c). Consistent with our design, gas vesicles purified from *arg2*-expressing *E. coli* had a lower critical hydrostatic collapse pressure